JACS
JOURNAL OF THE AMERICAN CHEMICAL SOCIETY

Communication

pubs.acs.org/JACS

Determining Molecular Orientations in Disordered Materials from X-ray Linear Dichroism at the Iodine L_1-Edge

Benjamin A. Palmer,[†] Stephen P. Collins,[‡] Jürg Hulliger,[§] Colan E. Hughes,[∥] and Kenneth D. M. Harris*[,∥]

[†]Department of Structural Biology, Weizmann Institute of Science, Rehovot 760001, Israel

[‡]Diamond Light Source, Harwell Science and Innovation Campus, Didcot, Oxfordshire OX11 0DE, England

[§]Department of Chemistry and Biochemistry, University of Bern, Freiestrasse 3, CH-3012 Bern, Switzerland

[∥]School of Chemistry, Cardiff University, Park Place, Cardiff CF10 3AT, Wales

Supporting Information

ABSTRACT: To demonstrate that measurements of X-ray linear dichroism are effective for determining bond orientations in disordered materials, we report the first observation of X-ray linear dichroism at the iodine L_1-edge. The iodine-containing molecular solid studied in this work was the inclusion compound containing 4,4′-diiodobiphenyl guest molecules in the perhydrotriphenylene host structure. In this material, the guest substructure does not exhibit three-dimensional ordering, and thus diffraction-based techniques do not provide insights on the orientational properties of the guest molecules. Iodine L_1-edge X-ray absorption spectra, recorded as a function of orientation of a single crystal of the material, exhibit significant dichroism (whereas no dichroism is observed at the iodine L_2- and L_3-edges). From quantitative analysis of the X-ray dichroism, the orientational properties of the C−I bonds within this material are established. The results pave the way for applying X-ray dichroism to determine molecular orientational properties of other materials, especially for partially ordered materials such as liquid crystals, confined liquids, and disordered crystalline phases, for which diffraction techniques may not be applicable.

While the interaction of linearly polarized visible light with anisotropic materials is well understood and widely exploited (e.g., in the polaroid sheet[1] and the polarizing optical microscope[2]), substantially less attention has been devoted to studies of the interaction of linearly polarized X-rays with materials. Recent studies of X-ray linear dichroism[3] and X-ray birefringence[4] have elucidated a deeper understanding of these phenomena, i.e., that the X-ray absorption coefficient (in the case of dichroism) and the refractive index (in the case of birefringence) of an anisotropic material depend on the orientation of the material relative to the direction of polarization of a linearly polarized incident X-ray beam. In the absence of diffraction, X-ray dichroism and X-ray birefringence are observed close to an absorption edge of a selected element within the material, arising due to local anisotropy in the bonding environment of the selected type of atom. Thus, unlike their optical analogues,[5] X-ray dichroism and X-ray birefringence are sensitive to the local orientational properties of individual molecules and chemical bonds, rather than the overall symmetry properties of the material.

The phenomena of X-ray dichroism and X-ray birefringence have the potential to be harnessed in a range of analytical techniques and devices. For example, solid inclusion compounds containing brominated organic molecules have been shown to function as effective X-ray dichroic filters.[3b,c] In this case, X-ray photons with polarization parallel to the C−Br bond axis in the material are preferentially absorbed over those with polarization perpendicular to this axis. Such dichroic filter materials have a range of potential applications, such as in polarization analysis of magnetic X-ray scattering[3b] and for X-ray polarimetry devices in astronomy. Measurements of X-ray birefringence have also been used to determine the orientational properties of specific bonds in solids.[4b,c] In particular, the X-ray birefringence imaging (XBI) technique,[4f,g] which represents the X-ray analogue of polarizing optical microscopy, enables measurements of X-ray birefringence to be carried out in a spatially resolved manner and yields information on the size, spatial distribution, and temperature dependence of orientationally distinct domains in materials.

Most previous research on X-ray dichroism and X-ray birefringence has focused on brominated organic materials using incident polarized X-rays at the bromine K-edge. To exploit the full potential of these phenomena and apply them to a wider range of problems in materials science, experiments at different absorption edges are required. In particular, on moving to elements of higher atomic number, the energy of the K-edge may be too high to be readily accessible at synchrotron facilities, and it is then relevant to explore the capability of using the lower-energy L-edges instead.

In pursuit of this goal, we report here the first studies of X-ray dichroism at the iodine L_1-edge; specifically, by studying the dependence of the X-ray absorption spectrum on the orientation of a single crystal of a material containing iodinated organic molecules, the orientational characteristics of the C−I bonds have been established. The material studied is a solid inclusion compound[6] containing 4,4′-diiodobiphenyl (DIBP; Figure 1a) guest molecules within the perhydrotriphenylene (PHTP; Figure 1b) host tunnel structure. Inclusion compounds of PHTP are

Received: August 29, 2016
Published: December 5, 2016

DOI: 10.1021/jacs.6b09054
J. Am. Chem. Soc. 2016, 138, 16188−16191

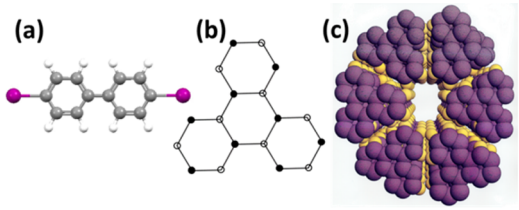

Figure 1. Molecular structures of (a) 4,4′-diiodobiphenyl (DIBP) and (b) perhydrotriphenylene (PHTP). (c) The tunnel host structure in PHTP inclusion compounds (guest molecules not shown).

constructed from stacks of PHTP molecules, forming one-dimensional (1-D) tunnels (Figure 1c) with elliptical cross-section (the van der Waals diameter of the tunnel is ∼4−7 Å, and the inter-tunnel separation is ∼14−15 Å). The PHTP host tunnel can accommodate a wide range of different types of guest molecule.[7] The specific physicochemical properties that result from the inclusion phenomenon may be exploited in a range of applications, such as "molecular reaction vessels" for stereo-selective polymerization reactions,[8] or as nonlinear optical[9] and pyroelectric[10] materials. PHTP inclusion compounds containing linear conjugated dyes as guest molecules can also perform efficient photon down-conversion and have potential uses in optoelectronic applications, including light-emitting diodes, photovoltaics, and silicon detectors.[11] We emphasize that several of these applications of PHTP inclusion compounds (or other types of solid inclusion compound) rely on exploiting the inclusion phenomenon as a strategy to *control* the orientational characteristics of the guest molecules; it is thus crucial that techniques are available to allow molecular orientational distributions in such materials to be established independently of X-ray diffraction (XRD) data, particularly when there is *positional* disorder of the guest molecules in the host structure.

Single-crystal XRD rotation photographs[12] of the DIBP/PHTP inclusion compound (recorded at ambient temperature) indicate that the X-ray scattering from the guest component comprises 2-D diffuse sheets in reciprocal space, from which it is concluded that the guest molecules are ordered only along each individual tunnel. Furthermore, there is an incommensurate relationship[13] between the periodicities of the host (c_h) and guest (c_g) substructures along the tunnel direction [c_g = 14.9(2) Å, c_h = 4.74(2) Å, $c_g/c_h \approx 3.14$]. In addition to the lack of 3-D positional ordering described above, the guest molecules in PHTP inclusion compounds can exhibit various other types of disorder,[14] such as dynamic disorder by reorientation about the axis of the host tunnel. Despite these aspects of disorder, the guest molecules may still have well-defined orientational properties relative to the PHTP host structure, as a consequence of the structural constraints imposed on the guest molecules by confinement within the host tunnel structure. Given that the guest substructure is only ordered in one dimension, and thus does not give sharp Bragg maxima in the single-crystal XRD pattern, alternative approaches are required to gain insights into the orientational characteristics of the guest molecules in these materials. Herein, we explore the opportunity to determine the orientational properties of the guest molecules in the DIBP/PHTP inclusion compound from iodine L_1-edge X-ray dichroism data.

X-ray absorption spectra were recorded in transmission at ambient temperature for a single crystal of the DIBP/PHTP inclusion compound on beamline I16 at Diamond Light Source,[15] using the setup in Figure 2 (full experimental details

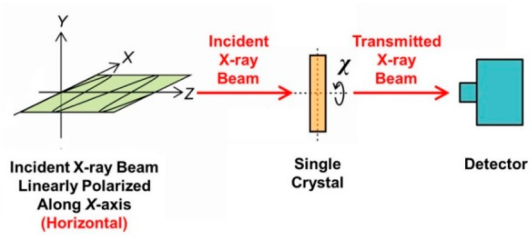

Figure 2. Experimental setup for X-ray dichroism studies. The incident X-ray beam propagates along the *z*-axis and is almost entirely linearly polarized along the *x*-axis. The crystal orientation angle χ is defined, with $\chi = 90°$ in the crystal orientation shown.

are given in the Supporting Information (SI)). The single crystal studied had a long-needle morphology (with distorted hexagonal cross-section) and overall dimensions 0.50 × 0.75 × 4.0 mm^3. Figure 3 shows the X-ray absorption spectra recorded in the

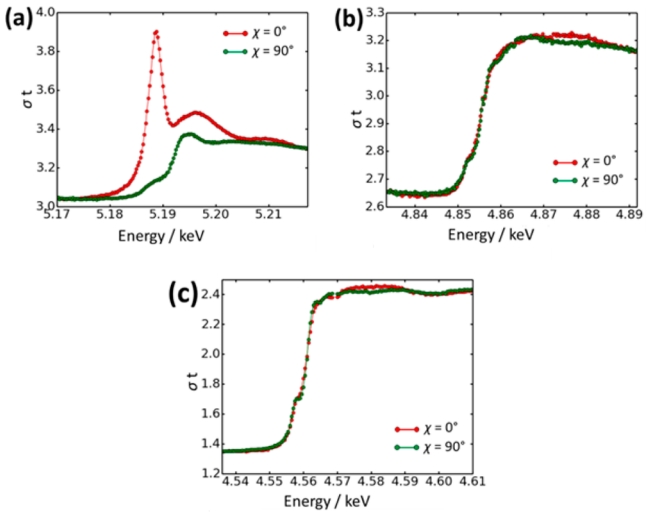

Figure 3. X-ray absorption spectra recorded for a single crystal of the DIBP/PHTP inclusion compound as a function of energy close to (a) the iodine L_1-edge, (b) the iodine L_2-edge, and (c) the iodine L_3-edge, with the tunnel axis of the PHTP host structure parallel ($\chi = 0°$; red data) or perpendicular (χ = 90°; green data) to the direction of linear polarization of the incident X-ray beam.

vicinity of the iodine L_1-, L_2-, and L_3-edges (spanning the energy range ∼4.5−5.3 keV), with the tunnel axis of the PHTP host structure (parallel to the long axis of the needle-shaped crystal morphology) oriented parallel (χ = 0°; red data in Figure 3) or perpendicular ($\chi = 90°$; green data in Figure 3) to the direction of linear polarization of the incident X-ray beam.

At the iodine L_1-edge (Figure 3a), the absorption of the linearly polarized X-rays depends strongly on crystal orientation, with highest absorption when the tunnel axis of the PHTP host structure is parallel to the direction of polarization of the incident X-ray beam (i.e., $\chi = 0°$), and significantly lower absorption when the tunnel axis is perpendicular to the direction of polarization of the incident X-ray beam (i.e., χ = 90°). The difference between the X-ray absorption spectra recorded for $\chi = 0°$ and 90° gives the X-ray dichroism data. The maximum X-ray dichroism arises at an incident X-ray energy of E = 5.188 keV.

As X-ray linear dichroism in the vicinity of the L_1-edge is dictated by the orientational characteristics of the C−I bonds in the material, our results suggests that the DIBP guest molecules are oriented with the C−I bonds close to parallel to the tunnel

DOI: 10.1021/jacs.6b09054
J. Am. Chem. Soc. 2016, 138, 16188−16191

axis of the PHTP host structure. The strong dichroic resonance observed at E = 5.188 keV arises from promotion of an iodine 2s core electron to the σ^* antibonding orbital associated with the C−I bond, which has mixed s-p character at the iodine site. The anisotropy of the X-ray absorption reflects the strong anisotropy of the σ^*(C−I) antibonding orbital. The probability of the 2s(I)→σ^*(C−I) transition depends strongly on the orientation of the vacant σ^*(C−I) antibonding orbital relative to the direction of linear polarization of the incident X-ray beam, and the highest transition probability arises when the C−I bond is parallel to the direction of polarization of the incident X-ray photons (i.e., for χ = 0°).

While our data at the iodine L_1-edge are consistent with the C−I bonds lying close to parallel to the tunnel axis of the PHTP host structure, a small peak is observed at E = 5.188 keV in the data recorded at χ = 90° (Figure 3a), suggesting that the C−I bond vector has a nonzero component in the plane perpendicular to the tunnel axis, such that the symmetry requirements for the 2s(I)→σ^*(C−I) transition are satisfied at χ = 90°, albeit with low probability. We suggest that this small peak arises from a slight tilting of the C−I bonds of the DIBP guest molecules away from the tunnel axis of the PHTP host structure.[16] As now described, quantitative analysis of the X-ray dichroism observed at the iodine L_1-edge allows the tilt angle ψ (defined in Figure 4) of the C−I bond with respect to the PHTP tunnel axis to be estimated.

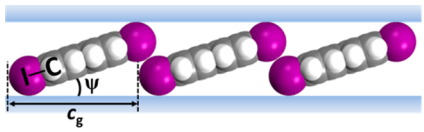

Figure 4. Schematic of the arrangement of DIBP guest molecules in the PHTP tunnel determined from quantitative analysis of the iodine L_1-edge X-ray dichroism data. The tilt angle (ψ) and periodic repeat distance (c_g) of the guest molecules are indicated.

We now consider geometric aspects (i.e., the orientation and polarization dependence) of X-ray linear dichroism at the iodine L_1-edge for iodinated organic materials containing C−I bonds. By applying the compact and powerful formalism of spherical tensors, we can build on results derived in the literature[3a,17] which provide a complete description of geometric properties of the X-ray absorption process, given a known set of tensor components. Our first task is to calculate the tensor components for the dipole absorption cross-section, based on the assignment that the sharp spectral line at E = 5.188 keV in the iodine L_1-edge spectrum arises from the 2s(I)→σ^*(C−I) transition, which occurs from an s-state to an empty antibonding orbital for which the p-projection lies along the C−I bond. Taking the quantization axis (z-axis) as the direction of the C−I bond, the initial-state and final-state wave functions are $|i\rangle \propto Y_0^0 = +1$ and $|f\rangle \propto Y_0^1 = [f_{-1}^1 f_0^1 f_{+1}^1] = [0,1,0]$.

All transitions thus correspond to zero change in the angular momentum projection, so (from eq 6.4 in ref 3a) we can select $\mu = \mu' = 0$, which leads to very simple expressions for the tensor components of the dipole absorption cross-section in terms of a single Clebsch−Gordon coefficient, $\sigma_Q^K = A(1,0,1,0|K,Q)$, where A is a constant factor that contains terms such as radial integrals. The nonzero values of σ_Q^K are $\sigma_0^0 = +A$ and $\sigma_0^2 = -\sqrt{2}A$, where σ_0^0 is a scalar and σ_0^2 is a quadrupole directed along the C−I bond. For the case in which the C−I bond lies in the plane perpendicular to the direction of propagation of the incident beam, and using θ to denote the angle between the photon polarization vector and the C−I bond, it can be shown (see eq 4.4 in ref 3a) that, assuming uniaxial anisotropy, the X-ray absorption coefficient has the following dependence on θ: $\sigma(\theta) \propto \cos^2\theta$.

In our experimental setup (Figure 2), the crystal orientation is specified by the angle χ between the tunnel axis of the PHTP host structure and the direction of polarization of the incident X-ray beam, whereas the equations above refer to the angle θ between the C−I bond and the direction of incident polarization. The fact that the peak at E = 5.188 keV is significantly more intense (Figure 3a) for χ = 0° than for 90° indicates that the orientation of the C−I bond must be close to the direction of the tunnel axis of the PHTP host structure. Nevertheless, the nonzero intensity observed for this peak at χ = 90° suggests that the C−I bond direction is tilted from the host tunnel axis. We incorporate this situation into a revised model[18] with the C−I bond tilted from the tunnel axis by an angle ψ and with disorder (dynamic or static) of the C−I bond by reorientation about the tunnel axis. In this model, the resultant disordered system is still uniaxial. The averaging due to disorder has no effect on the scalar part and does not introduce any new tensor components, and the only effect is to rescale the quadrupole term as $\sigma_0^2(\psi,\chi) = -(3\cos^2\psi - 1)/\sqrt{2}$, leading to a modified equation for the X-ray absorption coefficient: $\sigma(\psi,\chi) \propto 1 + (3\cos^2\psi - 1)(3\cos^2\chi - 1)/2$.

From this equation, the maximum X-ray absorption (at χ = 0°) is decreased and the minimum (at χ = 90°) is increased, relative to a situation in which the C−I bond is parallel to the tunnel axis (i.e., ψ = 0°). Consequently, the ratio of the X-ray absorption coefficients for the 90° (denoted $\sigma_\perp$) and 0° (denoted $\sigma_\parallel$) orientations is nonzero, and is given by $R = \sigma_\perp/\sigma_\parallel = {}^1/_2 \tan^2\psi$. From fitting the X-ray absorption spectra in Figure 3a (details of the fitting procedure are given in SI) to establish the ratio of the intensity of the peak at χ = 90° to the intensity of the peak at 0°, which is equal to the ratio of their absorption coefficients, $\sigma_\perp/\sigma_\parallel$, we obtain R = 0.0514, from which the (average) value of the tilt angle ψ is determined to be 17.8°. From the fitting procedure (see SI), the error in the value of R is ±0.006, leading to an estimated error in ψ of ~±1.0°.

This result demonstrates that analysis of X-ray linear dichroism data at the iodine L_1-edge may be exploited to determine the orientational properties of C−I bonds in disordered materials. In the case of the DIBP/PHTP inclusion compound (and other composite guest/host materials), such information cannot be obtained from XRD data due to the disordered nature of the guest molecules, encompassing both the lack of 3-D positional ordering and disorder with respect to guest molecules sampling different orientations (on either a static or dynamic basis) with respect to reorientation around the tunnel axis. Our conclusion that the axis of the DIBP guest molecule is tilted relative to the tunnel axis of the PHTP host structure is consistent with the fact that the reported[12] (from analysis of XRD rotation photographs) periodic repeat distance of the guest molecules along the tunnel [c_g = 14.9(2) Å] is *shorter* than the van der Waals length of the guest molecule (estimated 15.2 Å).

In contrast to the behavior at the iodine L_1-edge, no significant dichroism is observed at the L_2- or the L_3-edge (Figure 3b,c and SI). Thus, at the L_2- and L_3-edges, the X-ray absorption spectra are essentially identical for the χ = 0° and 90° orientations. The transitions at the L_2- and L_3-edges involve promotion of a 2p(I) electron to an empty s- or d-state, which occur in an essentially isotropic manner. We note that the absorption corresponding to the L_3-edge is twice the magnitude of that for the L_2-edge, as the L_3-edge originates from the degenerate $2p_x$ and $2p_y$ orbitals, whereas the L_2-edge originates from the $2p_z$ orbital. It is

DOI: 10.1021/jacs.6b09054
J. Am. Chem. Soc. 2016, 138, 16188−16191

noteworthy that the XANES regions of the iodine L_2- and L_3-edge X-ray absorption spectra are relatively "featureless" (compared to the L_1-edge X-ray absorption spectrum), consistent with previous observations for iodo-organic materials[19] and for molecular iodine and polyiodide anions in different environments.[20]

We have reported the first X-ray dichroism study at the iodine L-edges and have shown that measurements at the L_1-edge are an effective analytical method for determining C−I bond orientations in iodinated organic materials. This strategy is particularly useful when XRD techniques are not applicable, for example, in the case of materials that lack 3-D translational periodicity. Accessing the L_1-edge (rather than the higher-energy K-edge) allows such techniques to be applied to study elements of higher atomic number, and extends the opportunity to apply techniques based on polarized X-rays to a much wider range of materials. Thus, the results reported here pave the way for applying X-ray dichroism measurements to study the orientational properties of important iodine-containing materials, such as iodinated liquid crystals, halogen-bonded materials, polarizing films, X-ray contrast agents, and materials comprising self-assembled monolayers.[21] Another promising strategy to widen the scope of iodine L_1-edge X-ray dichroism is to dope non-iodine-containing materials with iodine (e.g., by iodo-substitution of organic molecules in place of F, Cl, Br, or H) to produce a dichroic probe that may be exploited to "report" on molecular orientation (in much the same way that tryptophans are engineered into proteins to study fluorescence anisotropy). Finally, we note that the strong X-ray dichroism exhibited by the DIBP/PHTP inclusion compound near the iodine L_1-edge suggests that this material could be used as an effective dichroic filter in X-ray polarization analysis.

■ ASSOCIATED CONTENT

Supporting Information

The Supporting Information is available free of charge on the ACS Publications website at DOI: 10.1021/jacs.6b09054.

Experimental details and fitting procedure used for quantitative analysis of X-ray dichroism data (PDF)

■ AUTHOR INFORMATION

Corresponding Author

*harriskdm@cardiff.ac.uk

ORCID

Kenneth D. M. Harris: 0000-0001-7855-8598

Notes

The authors declare no competing financial interest.

■ ACKNOWLEDGMENTS

We thank Diamond Light Source for beamtime on beamline I16, and the Human Frontiers Science Program (HFSP) for the award of a Cross-Disciplinary Postdoctoral Fellowship to B.A.P.

■ REFERENCES

(1) Land, E. H. *J. Opt. Soc. Am.* **1951**, *41*, 957.

(2) (a) Hartshorne, N. H.; Stuart, A. *Practical Optical Crystallography*; Edward Arnold Publisher: London, 1969. (b) Kaminsky, W.; Claborn, K.; Kahr, B. *Chem. Soc. Rev.* **2004**, *33*, 514.

(3) (a) Brouder, C. *J. Phys.: Condens. Matter* **1990**, *2*, 701. (b) Collins, S. P.; Laundy, D.; Harris, K. D. M.; Kariuki, B. M.; Bauer, C. L.; Brown, S. D.; Thompson, P. *J. Phys.: Condens. Matter* **2002**, *14*, 123. (c) Chao, M.-H.; Kariuki, B. M.; Harris, K. D. M.; Collins, S. P.; Laundy, D. *Angew. Chem., Int. Ed.* **2003**, *42*, 2982.

(4) (a) Templeton, D. H.; Templeton, L. K. *Acta Crystallogr., Sect. A* **1986**, *42*, 478. (b) Palmer, B. A.; Morte-Ródenas, A.; Kariuki, B. M.; Harris, K. D. M.; Collins, S. P. *J. Phys. Chem. Lett.* **2011**, *2*, 2346. (c) Palmer, B. A.; Edwards-Gau, G. R.; Morte-Ródenas, A.; Kariuki, B. M.; Lim, G. K.; Harris, K. D. M.; Dolbnya, I. P.; Collins, S. P. *J. Phys. Chem. Lett.* **2012**, *3*, 3216. (d) Joly, Y.; Collins, S. P.; Grenier, S.; Tolentino, H. C. N.; De Santis, M. *Phys. Rev. B* **2012**, *86*, 220101. (e) Collins, B. A.; et al. *Nat. Mater.* **2012**, *11*, 536. (f) Palmer, B. A.; Edwards-Gau, G. R.; Kariuki, B. M.; Harris, K. D. M.; Dolbnya, I. P.; Collins, S. P. *Science* **2014**, *344*, 1013. (g) Palmer, B. A.; Edwards-Gau, G. R.; Kariuki, B. M.; Harris, K. D. M.; Dolbnya, I. P.; Collins, S. P.; Sutter, J. P. *J. Phys. Chem. Lett.* **2015**, *6*, 561.

(5) Optical birefringence depends on the anisotropy of the material as a whole. For a crystalline material, it depends on the overall symmetry of the structure. For an ensemble of molecules or fibers, it may depend on the net orientational properties of the ensemble.

(6) (a) *Encyclopedia of Supramolecular Chemistry*; Atwood, J. L., Steed, J. W., Eds.; Marcel Dekker: New York, 2004; Vol. 2. (b) Harris, K. D. M. *Supramol. Chem.* **2007**, *19*, 47. (c) Palmer, B. A.; Harris, K. D. M.; Guillaume, F. *Angew. Chem., Int. Ed.* **2010**, *49*, 5096. (d) Palmer, B. A.; Le Comte, A.; Harris, K. D. M.; Guillaume, F. *J. Am. Chem. Soc.* **2013**, *135*, 14512.

(7) (a) Farina, M.; Di Silvestro, G.; Sozzani, P. In *Comprehensive Supramolecular Chemistry*; MacNicol, D. D., Toda, F., Bishop, R., Eds.; Pergamon: Oxford, 1996; Vol. 6, pp 371−398. (b) Couderc, G.; Hulliger, J. *Chem. Soc. Rev.* **2010**, *39*, 1545. (c) König, O.; Bürgi, H. B.; Armbruster, T.; Hulliger, J.; Weber, T. *J. Am. Chem. Soc.* **1997**, *119*, 10632.

(8) Farina, M.; Audisio, G.; Natta, G. *J. Am. Chem. Soc.* **1967**, *89*, 5071.

(9) (a) Hoss, R.; König, O.; Kramer-Hoss, V.; Berger, U.; Rogin, P.; Hulliger, J. *Angew. Chem., Int. Ed. Engl.* **1996**, *35*, 1664. (b) Hulliger, J.; König, O.; Hoss, R. *Adv. Mater.* **1995**, *7*, 719.

(10) (a) Hulliger, J. *Chem. - Eur. J.* **2002**, *8*, 4578. (b) Süss, H. I.; Wuest, T.; Sieber, A.; Althaus, R.; Budde, F.; Lüthi, H.-P.; McManus, G. D.; Rawson, J.; Hulliger, J. *CrystEngComm* **2002**, *4*, 432.

(11) (a) Botta, C.; et al. *Adv. Mater.* **2004**, *16*, 1716. (b) Aloshyna, M.; et al. *Adv. Funct. Mater.* **2008**, *18*, 915.

(12) König, O. Ph.D. Thesis, University of Bern, Switzerland, 1996.

(13) (a) Bak, P. *Rep. Prog. Phys.* **1982**, *45*, 587. (b) Rennie, A. J. O.; Harris, K. D. M. *Proc. R. Soc. London, A* **1990**, *430*, 615. (c) Sun, J.; Lee, S.; Lin, J. *Chem. - Asian J.* **2007**, *2*, 1204.

(14) (a) Mayo, S. C.; Proffen, T.; Bown, H.; Welberry, T. R. *J. Appl. Crystallogr.* **1999**, *32*, 464. (b) Weber, T.; Estermann, M. A.; Bürgi, H.-B. *Acta Crystallogr., Sect. B* **2001**, *57*, 579. (c) Sozzani, P.; Bovey, P. A.; Schilling, F. C. *Macromolecules* **1989**, *22*, 4225. (d) Schilling, F. C.; Sozzani, P.; Bovey, P. A. *Macromolecules* **1991**, *24*, 4369.

(15) Collins, S. P.; et al. *AIP Conf. Proc.* **2009**, *1234*, 303.

(16) In principle, this observation could be caused by slight misalignment of the single crystal such that, in the $\chi = 90°$ orientation, the tunnel axis is not perfectly perpendicular to the incident linear polarization. In our experiments (see SI for more details), accurate alignment was ensured by measuring diffraction data from the PHTP host structure using the diffractometer capability of beamline I16, then aligning the crystal with the tunnel axis strictly vertical for the measurement at $\chi = 90°$. X-ray absorption spectra were also measured for several different crystals; in all cases, the weak peak at $E = 5.188$ keV was observed at $\chi = 90°$, indicating that this peak is intrinsic in origin.

(17) Lovesey, S. W.; Balcar, E.; Knight, K. S.; Fernández Rodríguez, J. *Phys. Rep.* **2005**, *411*, 233.

(18) A similar model was developed previously[4g] in the context of an XBI study of a different solid inclusion compound.

(19) Schlegel, M. L.; Reiller, P.; Mercier-Bion, F.; Barré, N.; Moulin, V. *Geochim. Cosmochim. Acta* **2006**, *70*, 5536.

(20) Konishi, T.; Tanaka, W.; Kawai, T.; Fujikawa, T. *J. Synchrotron Radiat.* **2001**, *8*, 737.

(21) (a) Yu, Y.; Dubey, M.; Bernasek, S. L.; Dismukes, G. C. *Langmuir* **2007**, *23*, 8257. (b) Xiang, L.; Hines, T.; Palma, J. L.; Lu, X.; Mujica, V.; Ratner, M. A.; Zhou, G.; Tao, N. *J. Am. Chem. Soc.* **2016**, *138*, 679.

DOI: 10.1021/jacs.6b09054
J. Am. Chem. Soc. 2016, 138, 16188−16191